ISSN 1 746-7233, England, UK
World Journal of Modelling and Simulation
Vol. 10 (2014) No. 1, pp. 49-59

Numerical simulation of effects of machining parameters and tool geometry using DEFORM-3D: Optimization and experimental validation

T. Tamizharasan[1*], N. Senthilkumar[2]

[1] Principal, TRP Engineering College, Tiruchirappalli 621 105, India
[2] Adhiparasakthi Engineering College, Melmaruvathur, TamilNadu India-603319

(*Received November 21 2012, Accepted August 29 2013*)

Abstract. This research work focusses on optimization of machining and geometrical parameters during turning AISI 1045 steel using carbide cutting tool insert, by Finite Element Analysis and Taguchi's Technique. Three levels of cutting speed, feed rate, depth of cut, cutting insert shape, relief angle and nose radius are chosen. A suitable L18 Orthogonal array is selected based on Taguchi's Design of Experiments (DoE) and the simulation analysis is carried out using DEFORM-3D, machining simulation software and the output quality characteristics such as tool-chip interface temperature, interface pressure, wear depth, cutting forces and tool stress are analyzed by Signal-to-Noise (S/N) ratio. Analysis of Variance is performed to determine the most contributing factor, which shows that cutting insert shape is the most prominent parameter contributing by 37.84%, cutting speed by 13.47% and depth of cut by 11.56%. From the optimum condition evolved, validation is done experimentally and by FEM. It is observed that 18.81% increase in quality characteristics are achieved using the optimum condition.

Keywords: Tool geometry, flank wear, FEM analysis, Taguchi, DEFORM-3D

1 Introduction

Turning is a machining process for generating external surfaces of revolution by the action of a cutting tool on a rotating workpiece, done in a lathe. Cutting tool life is one of the most important economic considerations in metal cutting along with quality surface generated and cutting forces generated. In roughing operations, the tool material, the various tool angles, cutting speeds, and feed rates, are usually chosen to give an economical tool life. On the other hand, the use of very low speeds and feeds to give long tool life will not be economical because of the low production rate. The depth of cut should be as great as consistent with the strength and size of any cutting tool or carbide inserts when used, and the amount of stock to be removed. The feed depends on the desired finish and the strength and rigidity of the part and the machine. Cutting speed depends primarily on workpiece hardness and tool material[23].

By continually improving the carbide cutting tool insert geometries, the efficiency and effectiveness of machining process can be increased[20]. Machining a particular material under suitable conditions requires an optimal set of machining parameters and tool geometry[10]. The cutting life of carbide inserts can only be determined by cutting tests under real operating conditions. But model wear tests using finite element methods would be very much useful for the pre-selection of machining parameters and tool geometries. The main objective of this work is to study the effects of machining parameters such as cutting speed, feed rate, depth of cut and tool geometries such as cutting insert shape, relief angle and nose radius on flank wear[3], temperatures generated, cutting forces and stress on the inserts[12, 19]. The different shapes of inserts used for machining are shown in Fig. 1.

* Corresponding author. Tel.: +0431-2908050; fax: +0431-4298951. *E-mail address*: engineering91@gmail.com.

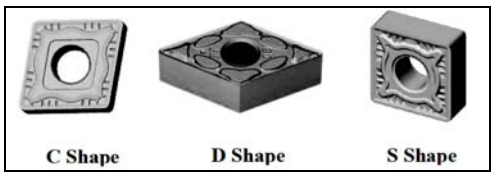

Fig. 1. Shapes of cutting inserts

Finite element simulation[8, 16] is carried out by varying the machining parameters[18] and tool geometries[9, 24, 27]. The cutting speed are chosen as 285 m/min, 256 m/min and 227 m/min, feed rate as 0.203 mm/rev, 0.318 mm/rev and 0.432 mm/rev and depth of cut as 0.3 mm, 0.45 mm and 0.6 mm and cutting inserts selected are C (Diamond 80º), D (Diamond 55º) and S (Diamond 90º) and relief angle as 0º, 3ºand 7ºand nose radius as 0.4 mm, 0.8 mm and 1.2 mm. For 6 parameters varied through 3 levels an L18 Orthogonal array is selected and the experiments are designed using Taguchi's Design of Experiment. Based on the designed L18 Orthogonal array, finite element simulation is carried out using commercially available DEFORM-3D software[13]. DEFORM is an engineering simulation software used by designers to analyze metal forming, machining and heat treatment processes by trial and error method. DEFORM is an effective tool for research and industrial applications. Many researchers have performed FEM analysis to study the effects of machining parameters for different materials. Based on the literature survey conducted, it is observed that no researcher has performed FEM analysis combining both the machining and geometrical parameters, as it is chosen in this present work. Researchers have considered different shapes of cutting insert having different nose radius separately only or its combination in limited. But in this research work, all parameters are considered for performing the FEM analysis.

The main contribution in this research work is to study the performance of carbide cutting tool inserts during turning AISI 1045 steel by varying the machining and geometrical parameters. The future scope is to study the effect of rake angle inclination and approach angle of cutting tools during machining with uncoated and coated inserts. Following the introduction part, the materials used as cutting insert and workpiece are given, followed by a brief introduction about the finite element method, with its need and cutting inserts modeled with meshing details. The technique used for analyzing the output parameter is described after it, followed by the simulation results obtained and a brief analysis of the results. Details of both FEM validation and experimental validation are provided and finally the results are concluded.

2 Materials for cutting insert and workpiece

The workpiece material used for the plane-strain orthogonal metal cutting simulation is AISI 1045 carbon steel whose chemical composition is given in Table 1. AISI 1045 is a low cost alloy with adequate strength and toughness suitable for most of the engineering and construction applications, whose Brinell hardness value is 181 HB. Engineering applications of AISI 1045 steel includes shafts, pins, bolts, gears, forgings, cold drawing and extrusion.

Table 1. Chemical composition of AISI 1045 steel

C	Si	Mn	Cr	Mo	Ti	V	W	P	S	Cu	Al	Fe
0.312	0.189	0.852	0.025	0.033	0.005	0.004	0.033	0.039	0.011	0.031	0.037	Remainder

The SEM image of AISI 1045 steel is shown in Fig. 2, which has large grains of pearlite in a matrix of ferrite. The microstructure is typical of medium carbon steel that has been hot rolled and re-crystallized. The flow line of the grains clearly shows the hot working operation carried out. The matrix is free from sulphide stringers which is a non-metallic inclusion. The grain size of the matrix is ASTM grain size No: 6 as per ASTM grain size measurement. The grain size is calculated as the average of five fields.

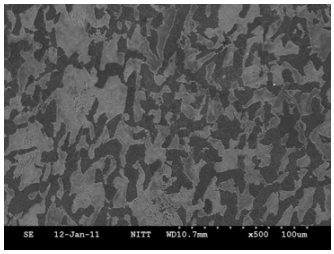

Fig. 2. SEM image of AISI 1045 steel

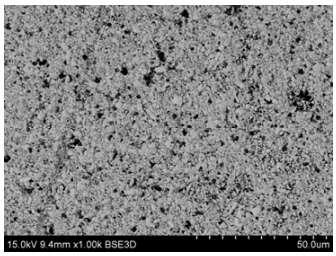

Fig. 3. SEM image of Cemented carbide insert

The cutting insert material used is uncoated Tungsten carbide [4] WIDIA make, whose material composition is given in Tab. 2.

Table 2. Chemical compositions of tungsten carbide insert

Tungsten carbide	Titanium carbide	Tantalum carbide	Molybdenum carbide	Cobalt
91∼93.2%	0.32%	0.89∼1.02	Traces	5.3∼6.1%

Fig. 3 shows the SEM image of cemented carbide insert in which the tungsten carbide particles are embedded in a matrix of titanium carbide, bonded by cobalt.

3 Finite element method

In recent years, finite element analysis[11, 15] has become the main tool for simulating orthogonal machining processes[6, 17]. Finite element analysis is preferred over experimental work because it saves time and cost. Moreover the results obtained from the finite element analysis stays close to the results obtained from the experimental work. Finite element method is proved to be an effective technique for analyzing chip formation processes and in predicting process variables such as temperatures, pressures[5, 26], forces and stresses etc. For our analysis, 18 different uncoated tungsten carbide cutting inserts are modeled using SOLIDWORKS, for various combination of cutting insert shape (included angle of insert), relief angle and nose radius. The modeled cutting tool inserts are shown in Fig. 4.

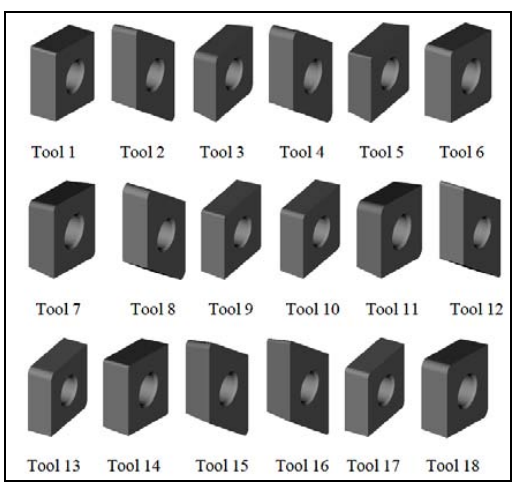

Fig. 4. Modeled cutting inserts used in FEM analysis

DEFORM-3D uses Usui's tool wear model to compute cutting insert wear, which can be used only with non-isothermal run as it requires interface temperature calculations. The initial temperature for the workpiece

and tool is set as 30ºC (room temperature). During meshing of cutting insert, the numbers of tetrahedron elements are fixed as 30000, while the number of elements in workpiece is kept at 25% of feed rate. A finer mesh can be seen at the tool tip and in the workpiece, where the tool comes in contact with the workpiece[1, 2]. The tetrahedral mesh of uncoated carbide insert and workpiece is shown in Fig. 5. The finite element analysis is carried out on a computer having a configuration of Intel core i3, M3502.27 GHz, 2 GB RAM with Windows 7, 32 bit operating system.

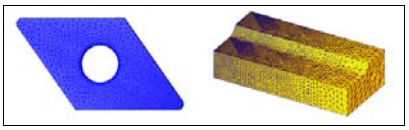

Fig. 5. Tetrahedral mesh of tool and workpiece

In Usui's tool wear model, given by Eq. (1), the wear rate is a function of constant pressure, relative velocity and absolute temperature at the contact surface. The constants of the wear rate model are taken as $A = 0.0000000078$ and $B = 5302$[25].

$$\frac{\mathrm{d}w}{\mathrm{d}t} = A\sigma_u V_s e^{(-B/T)}. \tag{1}$$

4 Taguchi's technique

The Taguchi method [14, 21] is a powerful tool in quality optimization. Optimization is carried out to utilize the available resources effectively to achieve better results[7, 22]. Taguchi method makes use of a special design of orthogonal array (OA) to examine the quality characteristics through a minimal number of experiments. The experimental results based on the orthogonal array are then transformed into S/N ratio to evaluate the performance characteristics. Taguchi design of experiments is used to design the orthogonal array for 6 parameters such as cutting speed, feed rate, depth of cut, cutting insert shape, relief angle and nose radius and for each parameter 3 different values that are chosen is shown in Tab. 3. The minimum number of experiments to be conducted for the parametric optimization is calculated as,

$$\text{Minimum experiments} = [(L-1)xP] + 1 = [(3-1)x6] + 1 = 13 \approx L18,$$

Table 3. Control Parameters and its Levels

Parameter/Level	Symbol	Level I	Level 2	Level 3
Cutting Speed (m/min)	A	227	256	285
Feed Rate (mm/rev)	B	0.432	0.318	0.203
Depth of Cut (mm)	C	0.3	0.45	0.6
Cutting Tool Insert Shape	D	C (80º)	D(55º)	S(90º)
Relief Angle (º)	E	0	3	7
Nose Radius (mm)	F	0.4	0.8	1.2

The various combinations of machining and geometrical parameters, designed using Taguchi's design of experiments, based on which the simulation analysis are to be conducted is shown in Tab. 4.

Based on the designed L18 Orthogonal array, finite element simulations are carried out and the response parameters like tool-chip interface temperature, interface pressure, wear depth, resultant cutting force and stresses acting on cutting tool are determined. The statistical measure of quality characteristic like Signal-to-Noise ratio is applied to analyze the effect of various machining parameters and cutting tool geometries on the output parameters. For analysis, there are 3 categories of performance characteristics, (i.e.) Smaller-the-better, Larger-the-better and Nominal-the-better.

Table 4. L_{18} Inner orthogonal array

Trial No	Cutting Speed (m/min)	Feed Rate (mm/rev)	Depth of Cut (mm)	Insert Shape	Relief Angle (°)	Nose Radius (mm)	ISO Insert Designation
1	227	0.432	0.3	C	0	0.4	CNMG 12 04 04
2	227	0.318	0.45	D	3	0.8	DAMG 15 04 08
3	227	0.203	0.6	S	7	1.2	SCMG 12 04 12
4	256	0.432	0.3	D	3	1.2	DAMG 15 04 12
5	256	0.318	0.45	S	7	0.4	SCMG 12 04 04
6	256	0.203	0.6	C	0	0.8	CNMG 12 04 08
7	285	0.432	0.45	C	7	0.8	CCMG 12 04 08
8	285	0.318	0.6	D	0	1.2	DNMG 15 04 12
9	285	0.203	0.3	S	3	0.4	SAMG 12 04 04
10	227	0.432	0.6	S	3	0.8	SAMG 12 04 08
11	227	0.318	0.3	C	7	1.2	CCMG 12 04 12
12	227	0.203	0.45	D	0	0.4	DNMG 15 04 04
13	256	0.432	0.45	S	0	1.2	SNMG 12 04 12
14	256	0.318	0.6	C	3	0.4	CAMG 12 04 04
15	256	0.203	0.3	D	7	0.8	DCMG 15 04 08
16	285	0.432	0.6	D	7	0.4	DCMG 15 04 04
17	285	0.318	0.3	S	0	0.8	SNMG 12 04 08
18	285	0.203	0.45	C	3	1.2	CAMG 12 04 12

$$\text{Smaller-the better (Minimize): } S/N = -10\log\left(\frac{1}{n}\sum_{i=1}^{n}\bar{y}_i^2\right), \tag{2}$$

$$\text{Larger-the better (Maximize): } S/N = -10\log\left(\frac{1}{n}\sum_{i=1}^{n}\frac{1}{\bar{y}_i^2}\right), \tag{3}$$

$$\text{Nominal-the best: } S/N = 10\log\left(\frac{\bar{y}}{s_y^2}\right). \tag{4}$$

For our objective, to obtain optimal machining performance, the smaller-the-better performance characteristic of output parameters should be chosen, as given by Eq. (2).

5 Simulation results and discussion

Finite element simulations are conducted to examine the effects of cutting speed, feed rate, depth of cut, cutting insert shape, relief angle and nose radius. After performing the simulation analysis, the output quality characteristics like tool-chip interface temperature, tool-chip interface pressure, wear depth, resultant cutting forces and tool stress are determined, which are tabulated in Tab. 5.

When the cutting speed increases, the chip temperature increases proportionately. The wear depth also increases with increase in cutting speed. Resultant cutting forces are lower when the cutting speed is low. When the feed rate increases, the chip temperature and tool-chip interface temperature increase with increase in wear depth. When feed rate is high, the cutting forces generated become higher. When depth of cut is high, the chip temperature and tool-chip interface temperature increase with increase in wear depth and cutting forces. When the included angle of the cutting insert is decreased, the chip temperature and tool-chip interface temperature become low with reduction in cutting forces. For maximum included angle, the wear depth is less, but the stress acting on the insert is high. When relief angle of the cutting insert is high, chip temperature increases with decrease in tool-chip interface temperature. Tool wear is low when relief angle is smaller. The

Table 5. Output quality characteristics of simulation analysis

Trial No	Tool-Chip Interface Tempt	Interface Pressure	Wear Depth	Cutting Force (N)				Tool Stress
	(ºC)	(MPa)	(mm)	F_X	F_Y	F_Z	Resultant	(MPa)
1	613	13800	$5.63E-08$	39.15	406.31	75.761	415.163	993
2	626	5390	$5.55E-08$	68.049	568.91	107.73	583.005	1380
3	565	8020	0.000000024	26.935	659.62	64.174	663.281	1580
4	616	8140	$5.75E-08$	37.987	378.16	64.17	385.442	955
5	704	32100	$8.07E-08$	29.191	803.5	81.633	808.164	2720
6	690	8560	$7.36E-08$	34.944	376.12	68.531	383.906	652
7	707	6000	0.000000107	96.196	783.28	169.09	807.077	1890
8	649	7100	$7.86E-08$	57.658	500.24	97.702	512.943	652
9	610	11100	$6.36E-08$	7.8598	424.88	37.283	426.585	1250
10	674	13900	0.000000099	38.768	936.42	113.12	944.024	1150
11	543	14300	$1.25E-08$	30.329	316.63	48.441	321.747	1590
12	648	11100	$6.92E-08$	81.191	576.45	117.12	593.804	877
13	682	51300	$9.28E-08$	28.374	772.01	108.47	780.109	909
14	725	13100	0.000000137	132	715.47	150.62	742.972	988
15	482	7080	$1.59E-08$	28.236	280.28	45.656	285.375	2140
16	715	11300	0.00000012	145.45	836.85	188.92	870.152	1070
17	679	25900	$4.65E-08$	11.847	518.41	65.618	522.681	1220
18	571	8300	$3.83E-08$	76.523	685.71	125.7	701.323	1500

stress acting on the insert is low when the relief angle is low. When the nose radius is high, the chip temperature, tool-chip interface temperature, wear depth and the cutting forces generated are lower with nominal stress acting on the cutting insert. Hence it is concluded that for machining AISI 1045 steel, the cutting speed and feed rate have to be minimum with a moderate depth of cut with a less included angle of cutting tool insert having a minimum relief angle and a larger nose radius. Since this is a simulation of turning process using FEM analysis, wear depth value achieved is lower. But in actual condition, the wear depth will be higher. This is due to the smaller mesh size at the tool-workpiece interface.

Using Minitab-16, statistical software, the analysis is carried out. Using the Smaller-the-better technique of Signal-to-Noise ratio the combined S/N ratio is determined, which is shown in Tab. 6.

Based on the determined combined S/N ratio the response table for cutting speed, feed rate, depth of cut, insert shape, relief angle and nose radius are determined by averaging the combined S/N ratio for each level of input parameters, as shown in Tab. 7.

From the response table, the main effects plot of S/N ratio is plotted for cutting speed, feed rate, depth of cut, cutting insert shape, relief angle and nose radius which are shown in Fig. 6.

From the response table and main effects plot of combined S/N ratio, the best level of parameters are identified as cutting speed of 285 m/min, feed rate of 0.203 mm/rev, depth of cut of 0.6 mm, cutting insert shape D (Diamond 55º), relief angle of 3ºand nose radius of 0.8 mm $(A_3B_3C_3D_2E_2F_2)$.

Analysis of Variance (ANOVA) is an important technique for analyzing the effect of categorical factors on a response. It is performed to determine the factors that contribute to the quality characteristics. Minitab-16, statistical software is used to perform the analysis. Table 8 shows the ANOVA table for the combined S/N ratio.

From the ANOVA table, it is observed that the cutting insert shape is the most significant factor contributing by 37.84%, followed by cutting speed by 13.47%, depth of cut by 11.56%. The contribution of other factors like feed rate, relief angle and nose radius are negligible.

Table 6. Combined S/N Ratio of the output quality characteristics

Trial No	Tool-Chip Temperature (ºC)	Interface Pressure (MPa)	Wear Depth (mm)	Resultant Cutting Force (N)	Tool Stress (MPa)	Combined S/N Ratio
1	613	13800	$5.63E-08$	415.163	993	−75.843
2	626	5390	$5.55E-08$	583.005	1380	−68.019
3	565	8020	0.000000024	663.281	1580	−71.308
4	616	8140	$5.75E-08$	385.442	955	−71.316
5	704	32100	$8.07E-08$	808.164	2720	−83.176
6	690	8560	$7.36E-08$	383.906	652	−71.721
7	707	6000	0.000000107	807.077	1890	−69.109
8	649	7100	$7.86E-08$	512.943	652	−70.13
9	610	11100	$6.36E-08$	426.585	1250	−73.991
10	674	13900	0.000000099	944.024	1150	−75.93
11	543	14300	$1.25E-08$	321.747	1590	−76.179
12	648	11100	$6.92E-08$	593.804	877	−73.971
13	682	51300	$9.28E-08$	780.109	909	−87.216
14	725	13100	0.000000137	742.972	988	−75.407
15	482	7080	$1.59E-08$	285.375	2140	−70.415
16	715	11300	0.00000012	870.152	1070	−74.153
17	679	25900	$4.65E-08$	522.681	1220	−81.291
18	571	8300	$3.83E-08$	701.323	1500	−71.581

Table 7. Response Table for combined S/N Ratio

Level / Parameter	Cutting Speed	Feed Rate	Depth of Cut	Insert Shape	Relief Angle	Nose Radius
Level 1	−73.54	−75.59	−74.84	−73.31	−76.7	−76.09
Level 2	−76.54	−75.7	−75.51	−71.33	−72.71	−72.75
Level 3	−73.38	−72.16	−73.11	−78.82	−74.06	−74.62

Table 8. Analysis of variance

Source	DOF	Seq SS	Adj MS	F	P	% Contribution
Cutting speed	2	12422674	6211337	3.04	0.137	13.47%
Feed rate	2	10332393	5166196	2.53	0.175	11.20%
Depth of cut	2	10663896	5331948	2.61	0.168	11.56%
Insert Shape	2	34896688	17448344	8.53	0.024	37.84%
Relief Angle	2	10379716	5189858	2.54	0.174	11.25%
Nose Radius	2	3309211	1654605	0.81	0.496	3.59%
Error	5	10226500	2045300			11.09%
Total	17	92231079				

5.1 Fem validation

With the identified optimum parameters, a new tool is modeled using SOLIDWORKS and a validation simulation analysis is performed and the quality characteristics obtained are shown in Tab. 9.

Fig. 7 shows the chip formation during machining AISI 1045 steel with the optimum machining and geometrical parameters along with graph showing the load acting on the cutting insert. It is observed that, the load acting on the insert is increased linearly with respect to time of the cutting tool comes in contact with the

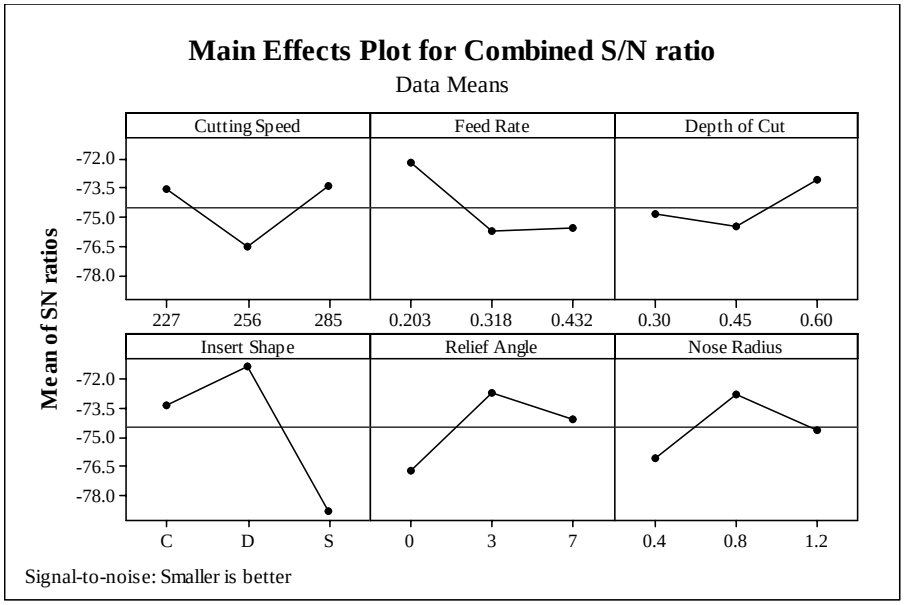

Fig. 6. Main effects plot for S/N ratio

Table 9. Output quality characteristics of optimal condition

Tool-Chip Temperature	Interface Pressure	Wear Depth	Cutting Force (N)				Tool Stress
(ºC)	(MPa)	(mm)	F_X	F_Y	F_Z	Resultant	(MPa)
689	7650	$8.47E-08$	65.375	524.38	93.086	536.576	1060

workpiece and after that during the machining process; the load acting on the cutting insert is stabilized with no more further increase in load.

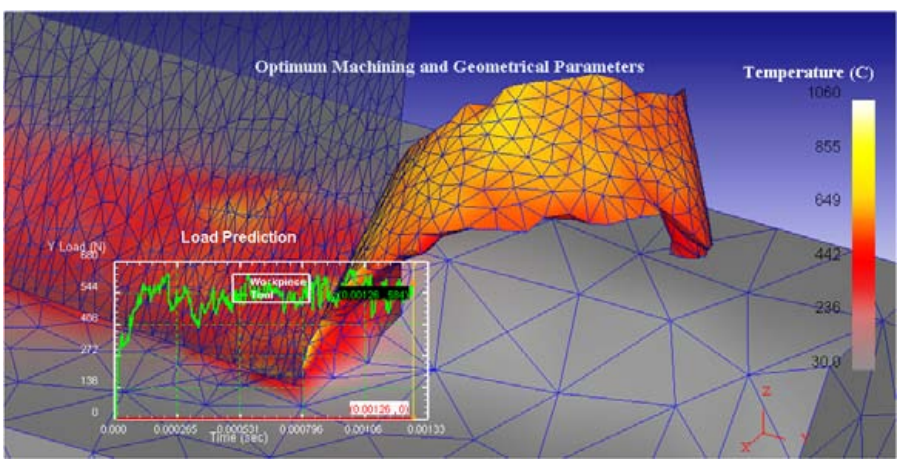

Fig. 7. Simulation result of optimum condition $A_3B_3C_3D_2E_2F_2$

The stress acting on the optimum cutting insert is shown in Fig. 8. The maximum stress acting is 760 MPa. It is also seen that the stress distribution is concentrated on the cutting edge of the cutting insert. Hence the cutting insert with less included angle will experience less stress than that of the cutting inset with more included angle.

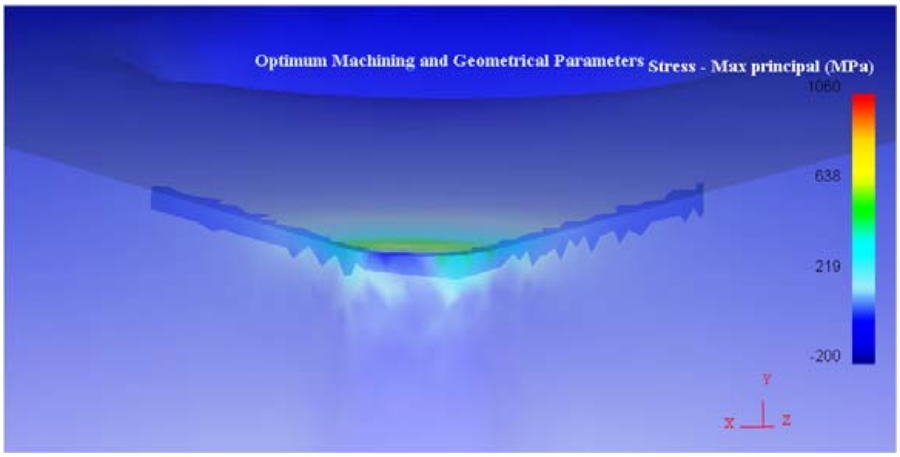

Fig. 8. Maximum principal stress in optimum insert

5.2 Experimental validation

Based on the obtained optimum condition an experiment is conducted in a CNC machine of specifications, Lokesh made 2 axis CNC TL-20, swing diameter 350mm, between center 600mm, spindle speed 4500 rpm, and the output parameters such as cutting forces is measured using a Kistler make tool dynamometer. Flank wear is measured by using a Mitutoyo digital tool makers microscope of specifications, eyepiece: 15X, view field diameter 13mm, objective 2X, working distance 67mm, total magnification 30X. Surface roughness is measured by using a Kosaka Laboratory Ltd make Surfcorder SE1200; with a vertical measuring range of 520μm, horizontal measuring range of 25mm, vertical resolution of 0.008μm, cutoff value of 0.8 mm with Gaussian filter.

The output results obtained are flank wear of 0.326 mm, surface roughness of 1.482 μm and cutting forces in x, y and z directions as 617.21 N, 276.41 N and 121.8 N with resultant cutting force of 687.16 N. Fig. 9 shows the surface roughness profile of the validated specimen, from which it is observed that the surface roughness pattern is uniform.

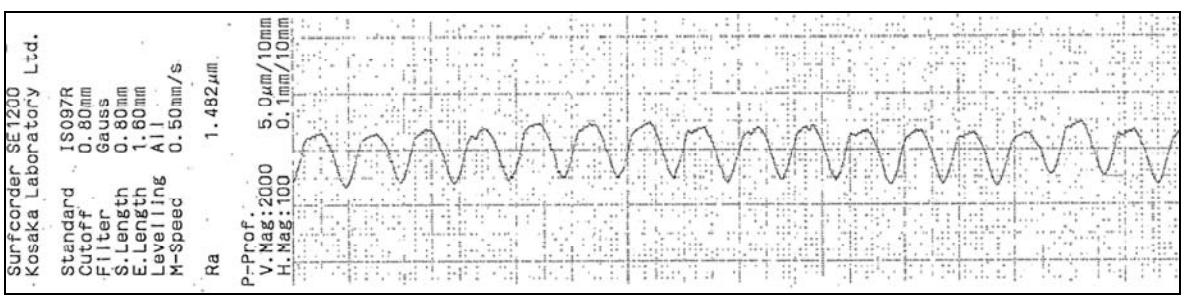

Fig. 9. Surface roughness profile of validation specimen

6 Conclusions

Performances of 18 ISO designated tools are analyzed during machining AISI 1045 steel by finite element simulation analysis using DEFORM-3D and optimized using Taguchi's technique. Experimental validation is done to verify the performance of optimum parameters. From analysis, it is concluded that,

(1) The optimum machining parameters obtained are cutting speed of 285 m/min, feed rate of 0.203 mm/rev and depth of cut of 0.6 mm.

(2) The optimum geometrical parameters obtained are cutting insert shape of D (Diamond 55º), relief angle

of 3ºand nose radius of 0.8 mm. i.e., DAMG 15 04 08.
(3) From Analysis of Variance, it is observed that the cutting insert shape is the most significant parameter contributing 37.84%, cutting speed by 13.47% and depth of cut by 11.56%. The contribution of feed rate, relief angle and nose radius are not that much significant.
(4) A decrease in output quality characteristics such as interface temperature, interface pressure, wear depth, resultant cutting force and tool stress by 18.81% is achieved by machining with the optimum tool and machining parameters.
(5) In future, the performance of coated carbide cutting tool with or without chip breakers can be analyzed. In addition, the influence of approach angle of cutting tool insert during turning may also be investigated.

References

[1] P. Arrazola, T. Ozel. Investigations on the effects of friction modeling in finite element simulation of machining. *International Journal of Mechanical Sciences*, 2010, **52**: 31–42.
[2] P. Arrazola, D. Ugarte, X. Dominguez. A new approach for the friction identification during machining through the use of finite element modeling. *International Journal of Machine Tools & Manufacture*, 2008, **48**: 173–183.
[3] A. Attanasio, E. Ceretti, et al. 3d finite element analysis of tool wear in machining. *CIRP Annals - Manufacturing Technology*, 2008, **57**: 61–64.
[4] A. Attanasio, E. Ceretti, et al. Investigation and fem-based simulation of tool wear in turning operations with uncoated carbide tools. *Wear*, 2010, **269**: 344–350.
[5] O. Beg, O. Makinde, et al. Hydromagnetic viscous flow in a rotating annular high-porosity medium with nonliner forchheimer drag effects: numerical study. *World Journal of Modelling and Simulation*, 2012, **8**(2): 83–95.
[6] H. Bil, S. Kilic, A. Tekkaya. A comparison of orthogonal cutting data from experiments with three different finite element models. *International Journal of Machine Tools & Manufacture*, 2004, **44**: 933–944.
[7] K. Deep, K. Das. Optimization of infiltration parameters in hydrology. *World Journal of Modelling and Simulation*, 2008, **4**(2): 120–130.
[8] C. Duan, T. Dou, et al. Finite element simulation and experiment of chip formation process during high speed machining of aisi 1045 hardened steel. *International Journal of Recent Trends in Engineering*, 2009, **1**(5): 46–50.
[9] K. Ee, O. Jr, I. Jawahir. Finite element modeling of residual stresses in machining induced by cutting using a tool with finite edge radius. *International Journal of Mechanical Sciences*, 2005, **47**: 1611–1628.
[10] V. Gaitonde, S. Karnik, J. Davim. Selection of optimal mql and cutting conditions for enhancing machinability in turning of brass. *Journal of Materials Processing Technology*, 2008, **204**: 459–464.
[11] K. Karanth, N. Sharma. Numerical analysis on the effect of varying number of diffuser vanes on impeller—diffuser flow interaction in a centrifugal fan. *World Journal of Modelling and Simulation*, 2009, **5**(1): 63–71.
[12] Q. Li, M. Hossan. Effect of cutting force in turning hardened tool steels with cubic boron nitride inserts. *Journal of Materials Processing Technology*, 2007, **191**: 274–278.
[13] R. Li, A. Shih. Finite element modeling of 3d turning of titanium. *International Journal of Advanced Manufacturing Technology*, 2006, **29**: 253–261.
[14] Y. Liu, W. Chang, Y. Yamagata. A study on optimal compensation cutting for an aspheric surface using the taguchi method. *CIRP Journal of Manufacturing Science and Technology*, 2010, **3**: 40–48.
[15] D. Maneetham, N. Afzulpurkar. Modeling, simulation and control of high speed nonlinear hydraulic servo system. *World Journal of Modelling and Simulation*, 2010, **6**(1): 27–39.
[16] C. Maranhao, J. Davim. Finite element modelling of machining of aisi 316 steel: Numerical simulation and experimental validation. *Simulation Modelling Practice and Theory*, 2010, **18**: 139–156.
[17] M. Miguelez, A. Sanchez, et al. An efficient implementation of boundary conditions in an ale model for orthogonal cutting. *Journal of Theoretical and Applied Mechanics*, 2009, **47**: 599–616.
[18] E. Oberg, F. Jones, et al. *Machinery's Handbook 28th Edition*. Industrial Press, New York, 2008.
[19] T. Ozel, T. Altan. Determination of workpiece flow stress and friction at the chip-tool contact for high-speed cutting. *International Journal of Machine Tools & Manufacture*, 2000, **40**: 133–152.
[20] T. Ozel, M. Sima, et al. Investigations on the effects of multi-layered coated inserts in machining ti-6al-4v alloy with experiments and finite element simulations. *CIRP Annals - Manufacturing Technology*, 2010, **59**: 77–82.
[21] G. Prihandana, M. Mahardika, et al. Effect of micro-powder suspension and ultrasonic vibration of dielectric fluid in micro-edm processes-taguchi approach. *International Journal of Machine Tools & Manufacture*, 2009, **49**: 1035–1041.
[22] K. Ramji, V. Goel, et al. Optimum design of suspension system of three-wheeled motor vehicles. *World Journal of Modelling and Simulation*, 2007, **3**(1): 36–44.

[23] G. Schneider, J. Cmfge. *Cutting Tool Applications*. GMRS Associates, 2002.

[24] Y. Yen, A. Jain, T. Altan. A finite element analysis of orthogonal machining using different tool edge geometries. *Journal of Materials Processing Technology*, 2004, **146**: 72–81.

[25] Y. Yen, J. Sohner, et al. Estimation of tool wear in orthogonal cutting using the finite element analysis. *Journal of Materials Processing Technology*, 2004, **146**: 82–91.

[26] X. Zhao, J. Xu. Numerical simulation of temperature and pressure distribution in producing gas well. *World Journal of Modelling and Simulation*, 2008, **4**(2): 94–103.

[27] J. Zouhar, M. Piska. Modelling the orthogonal machining process using cutting tools with different geometry. *MM Science Journal*, 2008, 49–51.